Journal of Magnetic Resonance **156,** 249–257 (2002)
doi:10.1006/jmre.2002.2563

Experiments to Detect Long-Range Heteronuclear Shift Correlations: LR-*J*-HSMQC

A. M. Torres,[1] W. A. Bubb, and P. W. Kuchel

School of Molecular and Microbial Biosciences, University of Sydney, Sydney, New South Wales 2006, Australia

Received December 7, 2001; revised May 6, 2002; published online July 3, 2002

The utility of the *J*-HSMQC experiment to detect long-range CH correlations was investigated. Two new long-range *J*-compensated pulse sequences, LR-*J*-HSMQC(80,27) and LR-*J*-HSMQC(27,80), were developed using the $(3\beta_x)\beta_y$ composite 90° pulse sequence. These two experiments were shown to be effective for long-range coupling constants, $^nJ_{CH}$, that were greater than 3 Hz. Although the overall sensitivities of the long-range *J*-HSMQC experiments were slightly lower than that of the conventional decoupled HMBC experiment, their 2D maps showed additional cross peaks that could be useful in structure elucidation. LR-*J*-HSMQC(27,80) was very efficient in yielding two- and four-bond relay correlations. The utility of the new sequences is demonstrated with strychnine as the sample.

***Key Words*: *J*-compensation; long-range correlation; HMBC; *J*-HSMQC; LR-*J*-HSMQC.**

INTRODUCTION

The heteronuclear multiple-bond correlation (HMBC) experiment introduced by Bax and Summers (*1*) has been one of the most versatile and indispensable tools in NMR spectroscopy for elucidating structures of small organic molecules including natural products. This 2D technique is useful in establishing long-range correlations between protons and carbons that are generally separated by two or three bonds.

Despite its usefulness, the HMBC experiment has a number of inadequacies that have attracted the interest of various workers in the field of pulse sequence development (*2–7*). One is the impossibility to cover a wide range of long-range coupling constants, which can span 1 to 25 Hz, in a single HMBC experiment. One approach to resolving this problem is to perform a series of experiments in which the delay, τ, that is used for scalar coupling evolution, is varied (*2*). This experiment, ACCORD-HMBC, employs carbon decoupling and purge pulses to remove direct $^1J_{CH}$ responses. However, the cross peaks have an undesirable skewed lineshape that is caused by homonuclear coupling in f_1 (*3*). Constant time versions of this sequence have since been introduced to improve the quality of the resulting spectra (*4, 5*). In another approach, 3D-HMBC (*6*), τ delay periods are incremented so that each of the appropriate slices in a pseudo 3D experiment corresponds to a 2D HMBC with a specific value of τ. The objective here is that most of the *J* values will be sampled by the numerous τ periods employed. The drawbacks of this method, of course, are the large size of the resulting data sets and the increased time required for analysis of 3D data sets compared with their 2D counterparts.

Modifications to the basic HMBC pulse sequence by several groups have addressed some of the other inadequacies. Furihata and Seto (*7*), for example, showed that the sensitivity can be increased by refocusing the antiphase signal and decoupling the carbon nuclei, notwithstanding extra signal loss due to transverse relaxation that occurs during the added delay. This pulse sequence, referred to as decoupled HMBC (D-HMBC), is equivalent to the heteronuclear multiple-quantum-coherence experiment (HMQC) with delays optimized for long-range coupling.

In this study, we investigated the use of the *J*-compensated heteronuclear shift correlation experiment, *J*-HSMQC (*8*), as a time-efficient alternative method for observing proton–carbon long-range correlations. *J*-HSMQC was originally introduced to address the wide variations in the magnitude of one bond proton to carbon spin–spin couplings. This *J*-compensated sequence differs from conventional heteronuclear single-bond correlation sequences in that it simultaneously detects both multiple- and single-quantum coherences that evolve during t_1. As with D-HMBC, carbon decoupling can also be performed during acquisition.

THEORY

Background

J-compensated pulse sequences are magnetization transfer experiments created from composite RF pulses by using the formal evolution-operator relationships that exist between spin–spin coupling and RF pulses as they act on spin systems (*9*). Composite pulses that are efficient in the presence of B_1-field inhomogeneity lead to *J*-compensated sequences that are more effective over a wide range of *J* values. *J*-compensation is achieved when these elements are used to replace the simple τ delay period for spin–spin coupling evolution in any existing pulse method.

[1] To whom correspondence should be addressed. E-mail: A.Torrres@biochem.usyd.edu.au.

1090-7807/02 $35.00

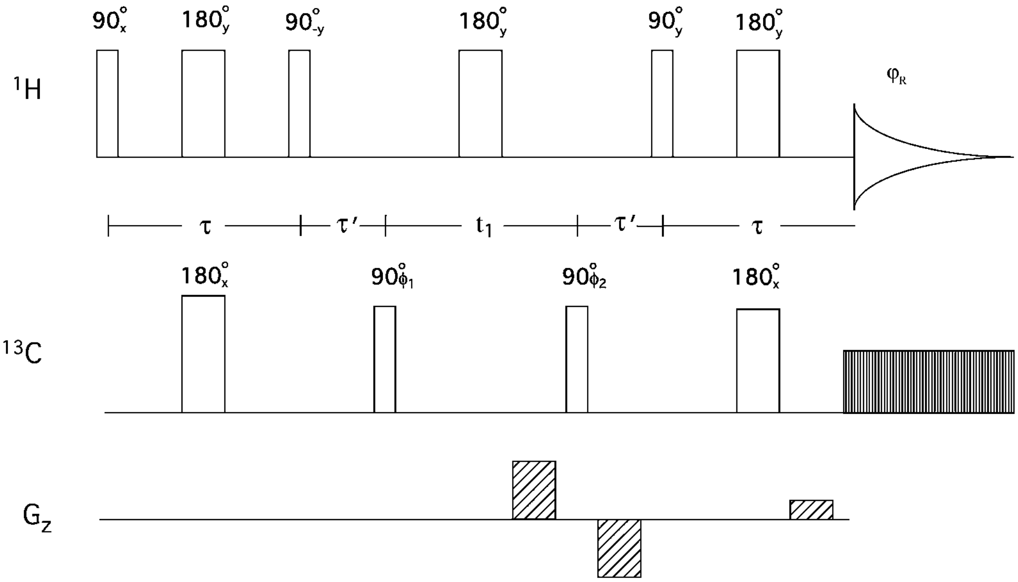

FIG. 1. Pulse sequence for J-HSMQC and LR-J-HSMQC. For observing direct CH correlations, the delays τ and τ' are set equal to $1/(2^1 J_{CH}^{nom})$. For observing long-range CH correlations, the delays τ and τ' are set to appropriate values: for LR-J-HSMQC(80,27), $\tau = 80$ ms and $\tau' = 27$ ms; for LR-J-HSMQC(27,80), $\tau = 27$ ms and $\tau' = 80$ ms. The gradient ratios of $40:-40:10$ select both multiple-quantum and single-quantum coherences that are present during the t_1 period. $\phi_1 = x\ -x\ x\ -x$; $\phi_2 = x\ x\ -x\ -x$; $\varphi_R = x\ -x\ -x\ x$.

Examples of conventional NMR experiments that can be modified for J-compensation include APT (*10*), INEPT (*11*), DEPT (*9*), and INADEQUATE (*12*).

The J-HSMQC sequence, as shown in Fig. 1, is patterned on composite pulses that nutate z-magnetization to the transverse plane more effectively than a single 90° RF pulse that may have B_1-field inhomogeneity or be miscalibrated. The pulse sequence of J-HSMQC is similar to the HSQC sequence except for the two extra delays, τ', which are made equal in magnitude to τ. We introduce here the long-range version of J-HSMQC in which the delays τ and τ' were adjusted to match long-range couplings instead of direct coupling, as presented originally (*8*). We also added gradient pulses to the J-HSMQC sequence to select required coherences directly, thereby removing unwanted t_1 noise that is commonly associated with inverse proton-detected experiments.

The mechanics of the J-HSMQC experiment for one bond correlation have been described fully elsewhere (*8*) and are only discussed briefly here. During the first τ period, nominally set to $1/(2^1 J_{CH}^{nom})$ in the J-HSMQC sequence, transverse proton magnetization $-H_y$ is transformed principally into anti-phase magnetization $2H_xC_z$. If τ deviates significantly from $1/(2^1 J_{CH}^{nom})$, which is normally the case, some $-H_y$, that is referred to as the ancillary component, remains unconverted. The 90°_{-y} proton pulse does not affect the ancillary $-H_y$ component; however, it "stores" the principal $2H_xC_z$ into longitudinal spin order $2H_zC_z$ so that it remains invariant during the τ' period. The purpose of the extra delay τ' is essentially to give the ancillary $-H_y$ a "second chance" to evolve into $2H_xC_z$. The application of the first 90°_x carbon pulse transforms the principal $2H_zC_z$ into anti-phase $-2H_zC_y$ while the ancillary $2H_xC_z$ is converted into multiple-quantum coherence $-2H_xC_y$. Both principal and ancillary components are labelled by the carbon chemical shift during t_1 and both are detected during acquisition. This is in stark contrast to the conventional HMQC or HSQC experiments where only the principal component is detected. The transformations of coherences after t_1 in J-HSMQC are just the reverse of what is described above.

It is clear that the J-compensation in the J-HSMQC experiment is due to the "storing" of the principal component, and the additional τ' delay period allows the mismatched ancillary magnetization to be converted into desirable coherences. If relaxation, homonuclear proton coupling, and pulse imperfections are neglected, it can be seen that the intensity of the signal, or cross peak, in J-HSMQC is proportional to $\sin^2(\pi^1 J_{CH}\tau) + \cos^2(\pi^1 J_{CH}\tau)\sin^2(\pi^1 J_{CH}\tau')$ which is the addition of the signal from the principal and ancillary components, respectively. Note that the signal intensity profile for D-HMBC (or HMQC) is proportional to the principal J-HSMQC component intensity which is $\sin^2(\pi^1 J_{CH}\tau)$. Clearly, the effectiveness of the compensated sequence is due to the extra $\cos^2(\pi^1 J_{CH}\tau')\sin^2(\pi^1 J_{CH}\tau')$ term from the ancillary component. This basically means that the second τ' period provides additional J-coupling evolution for magnetization which is otherwise lost in a conventional experiment.

In the original J-HSMQC sequence, the τ' period is set equal to τ' implying an analogy with a $\beta_x\beta_y$ composite pulse. Other composite pulse trains may be used to create J-compensated sequences so that τ and τ' delays need not be equal in magnitude. In principle, the order of τ and τ' may be reversed without

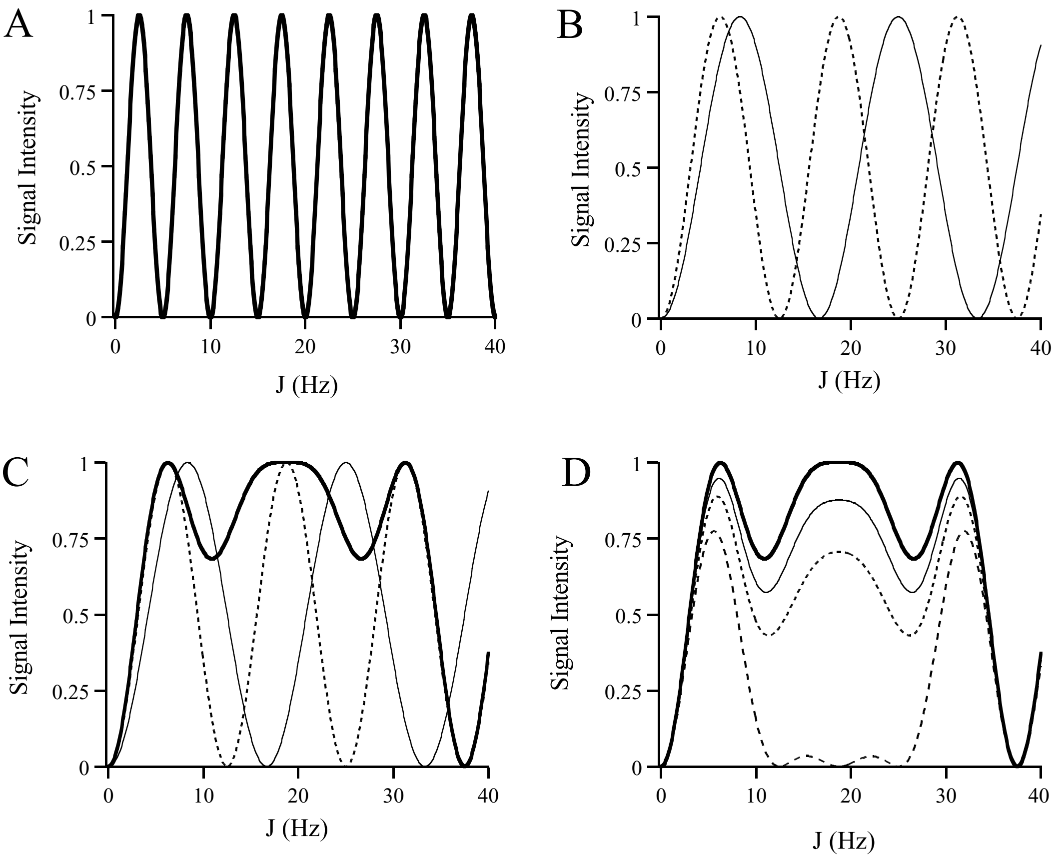

FIG. 2. Theoretical performance of D-HMBC and LR-J-HSMQC(80,27) experiments as functions of long-range coupling constants $^nJ_{\mathrm{CH}}$. (A) D-HMBC(200), (B) D-HMBC(60) (light solid line) and D-HMBC(80) (dotted line), (C) LR-J-HSMQC(80,27) (heavy solid line), D-HMBC(60) (light solid line), and D-HMBC(80) (dotted line), (D) LR-J-HSMQC(80,27) with $^nJ_{\mathrm{HH}}$ equal to 0 Hz (heavy solid line), 2.0 Hz (light solid line), 3.1 Hz (dotted lined), and 6.2 Hz (dashed line).

compromising the performance of J-HSMQC. This is because the signal intensity profile of the J-compensated cross peaks mentioned above can be rearranged so that they are proportional to $1 - \cos^2(\pi\,^1J_{CH}\tau)\cos^2(\pi\,^1J_{CH}\tau')$. However, note that the difference in relaxation rates of various coherences involved at different stages of the sequence, such as $2H_zC_z$, H_y, and $2H_xC_y$, will have an effect on the performance of a particular J-HSMQC sequence. Moreover, the contribution of homonuclear coupling, which is known to produce relay-type cross peaks in J-HSMQC (*8*), will also be different if the order of τ and τ' is reversed.

Development of Long-Range *J*-HSMQC

In developing the long-range J-HSMQC experiment, we compared its performance with the D-HMBC sequence instead of the conventional HMBC since both J-HSMQC and D-HMBC experiments employ carbon refocusing and decoupling. For these two experiments (or for many long-range heteronuclear correlation experiments), the acquired proton signals are actually phase-modulated by homonuclear coupling so that they are more conveniently displayed in magnitude mode. To simplify the evaluation of the J-compensated sequence we did not include the purging pulses that remove cross peaks which result from one bond spin-coupling interactions, but purging pulses may be easily incorporated into the sequence if required.

Figures 2A and 2B present the theoretical performance of the D-HMBC experiment with various delay periods as functions of the long-range coupling constant $^nJ_{\mathrm{CH}}$. The inefficiency of the conventional long-range experiment in the presence of a wide range of $^nJ_{\mathrm{CH}}$ values is clearly illustrated in the figures. As shown in Fig. 2A, setting τ to 200 ms for D-HMBC maximizes the signals for which $^nJ_{\mathrm{CH}} = 2.5$ Hz, but this condition totally eliminates signals for $^nJ_{\mathrm{CH}}$ values of 5, 10, 15, 20, and 25 Hz. Thus it is not generally advisable to set τ to very long values in a conventional long-range shift correlation experiment because, besides causing signal loss due to relaxation, there will be unwanted modulation of signal intensities for many $^nJ_{\mathrm{CH}}$ values. In practice, τ is usually set to between 60 and 80 ms in a regular HMBC experiment (Fig. 2B) to cover a range of $^nJ_{\mathrm{CH}}$ values. It can be seen that the D-HMBC experiments with τ set to either of these limits, D-HMBC(60) and D-HMBC(80), perform considerably better than that in which τ is set to 200 ms, because no null is expected for $^nJ_{\mathrm{CH}}$ below ∼10 Hz. However, these two conditions are still associated with appreciable signal attenuation for commonly encountered values of ${}^{n}J_{CH}$. In D-HMBC(80), signals with ${}^{n}J_{CH}$ values from 0–3.1, 9.5–15.6, and 21.9–28.1 Hz are less than 50% of the theoretical maximum. In addition, signals in which ${}^{n}J_{CH}$ is 12.5 and 25.0 Hz are nulled, so that corresponding cross peaks should not be expected in the 2D spectrum. For D-HMBC(60), signals for which ${}^{n}J_{CH}$ values are between 0–4.1 and 12.5–20.8 Hz are 50% or less than the theoretical maximum.

A *J*-compensated sequence affords the possibility of providing a more uniform signal response over an extended range of ${}^{n}J_{CH}$. Composite pulses that can be used as the basis of *J*-compensated proton-detected sequences are those that efficiently nutate *z*-magnetization to the transverse plane in the presence of B_1-field inhomogeneity (*8*). These composite pulses should have short durations so that corresponding *J*-compensated sequences are also relatively short and therefore less prone to the adverse effects of relaxation. Obvious candidates are the $(2\beta)_x\beta_y$ (where β is nominally 90°) composite pulse train which is implemented in CAPT3 (*10*) and $\beta_x\beta_y$ which is used in *J*-HSMQC (*8*).

Figure 3 shows the theoretical performance of the D-HMBC and *J*-HMQC sequences for various composite pulses as functions of $\beta' = \pi {}^{n}J_{CH}\,\tau$. Since the length of the second pulse in the composite pulse train is related to the length of the first pulse, the τ' delay period is dependent on the τ delay by a scalar factor. This leads to expected signal intensities that depend only on τ and ${}^{n}J_{CH}$. One can see that the *J*-compensated sequence based on $(2\beta)_x\beta_y$ is distinctly better than that based on $\beta_x\beta_y$ because it yields higher signal intensities for a wider range of β' values. For $\beta' = 45°$, the compensated sequence created from $(2\beta)_x\beta_y$ yields maximum intensity while the one based on $\beta_x\beta_y$ and D-HMBC (β_x) give 75 and 50% of the maximum signal, respectively. The *J*-compensated sequence patterned after a $(3\beta)_x\beta_y$ composite pulse gives the widest excitation profile among the three sequences, yielding optimal excitation for $\beta' =$ 30°, 90°, 150°, although there are two local minima at $\beta' = 52°$ and $\beta' = 128°$.

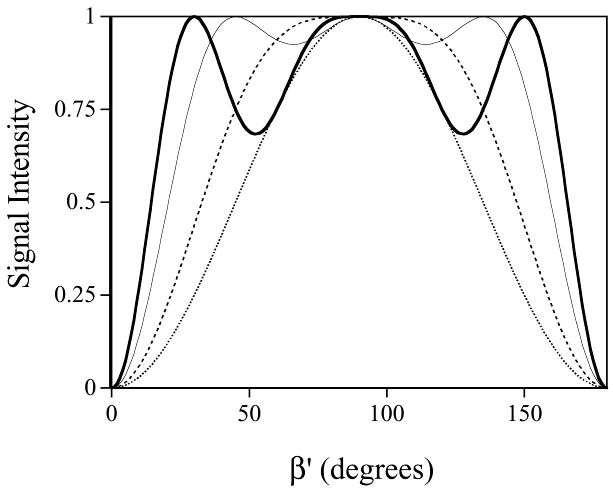

FIG. 3. Theoretical performance of D-HMBC and various *J*-HSMQC experiments as functions of flip angle $\beta' = \pi {}^{n}J_{CH}\,\tau$ expressed in degrees. D-HMBC described by β alone (dotted line); *J*-HSMQC patterned from $\beta_x\beta_y$ (dashed line), $(2\beta)_x\beta_y$ (thin solid line), $(3\beta)_x\beta_y$ (thick solid line).

It appears that the $(3\beta)_x\beta_y$ composite pulse leads to a long-range *J*-HSMQC that is considerably longer in duration than the conventional D-HMQC or the long-range *J*-HSMQC sequence patterned on the $(2\beta)_x\beta_y$ composite pulse. However, in choosing a τ delay period for the compensated *J*-HSMQC experiment, one also has to consider the efficiency of the *J*-compensated sequence. Specifically, in improving D-HMBC with τ set to 80 or 60 ms, we can set $\tau = 80$ and $\tau' = 27$ ms to create the long-range *J*-compensated sequence, LR-*J*-HSMQC(80,27), patterned on the $(3\beta)_x\beta_y$ composite pulse; a long-range *J*-HSMQC experiment based on a $(2\beta)_x\beta_y$ composite pulse train can be obtained by setting $\tau = 80$ and $\tau' = 40$ ms [LR-*J*-HSMQC(80,40)]. Note that the duration of the LR-*J*-HSMQC(80,27) sequence is only 34% longer than that of the D-HMBC(80) while the duration of the LR-*J*-HSMQC(80,40) is 50% longer. It is clear that LR-*J*-HSMQC(80,27) is both more efficient and shorter LR-*J*-HSMQC(80,40).

The efficiency of LR-*J*-HSMQC(80,27) as a function of ${}^{n}J_{CH}$ is presented in Fig. 2C. This *J*-compensated experiment is truly remarkable because it has no null below 37 Hz and is actually 68%, or more, efficient for ${}^{n}J_{CH}$ between 3.8–33.7 Hz. Although this sequence has two minima near ${}^{n}J_{CH}$ equal to 10.9 and 26.6 Hz, the excitation efficiency of ~68% at these two regions is still satisfactory. It is evident that LR-*J*-HSMQC(80,27) covers all potential long-range ${}^{n}J_{CH}$ values above 3 Hz.

Presence of Relay Peaks in *J*-HSMQC and LR-*J*-HSMQC

One attribute of *J*-HSMQC that may be beneficial is its ability to display relay cross peaks (*8*). This is achieved when the second τ' delay allows the δ_C-labelled ancillary $2H_xC_z$ magnetization to evolve under homonuclear H–H and one-bond heteronuclear H–C scalar couplings into $2H_xH_z^R$ (where H^R represents the remote proton) so that the last 90° H_y pulse converts this magnetization into $2H_zH_x^R$. This, in effect, transfers magnetization from a carbon with a directly attached proton to a remote proton, without undergoing direct heteronuclear H–C scalar coupling.

It is possible therefore that through a similar relay mechanism, correlations with very small long-range ${}^{n}J_{CH}$ values, or even none at all, may appear in the LR-*J*-HSMQC 2D spectrum. In essence, LR-*J*-HSMQC acts like two heteronuclear experiments, a long-range and a relay, combined into one experiment, with *J*-compensation added as a bonus. Normally, relay peaks are observed between a proton and carbon that are separated by only two bonds (*13*). Since the two delays, τ and τ', in the LR-*J*-HSMQC experiment are of the order of tens of milliseconds, magnetization transfer through a relay mechanism can effectively be achieved between protons and carbons separated by up to four bonds. It may be argued that the presence of relay peaks in the long-range heteronucelar correlation only complicates the analysis; thus it may be perceived that this is a major drawback of LR-J-HSMQC. However, there are instances when this information is useful in establishing connectivities. To increase the number of two-bond relay peaks and their intensities in LR-J-HSMQC spectra, the first τ delay should be as short as possible so that more ancillary magnetization $-H_y$ remains and this can undergo proton–proton coupling evolution during the τ' delay periods. As noted above, reversing the order of τ and τ' in the J-HSMQC sequence should not, in principle, affect the efficiency of the J-compensation for an isolated two-spin CH system where homonuclear coupling is absent. It is therefore expected that the reverse sequence LR-J-HSMQC(27,80) would produce more relay peaks than LR-J-HSMQC(80,27), especially for those systems where homonuclear couplings are significant.

It is important to note that although the homonuclear coupling results in relay peaks that may be desirable, this coupling interaction, in fact, degrades the performance of the LR-J-HSMQC. This contrasts with the D-HMBC profile which is unaffected by homonuclear coupling. Figure 2D shows the profile of LR-J-HSMQC(80,27) in the presence of different values of the homonuclear coupling constant $^nJ_{H1H2}$. For simplicity, only one proton coupling partner is considered; no heteronuclear H–C coupling with the second proton is assumed, and only the signal from the first proton is plotted. Clearly, there is a decrease in the total signal intensity and J-compensation with increasing values of $^nJ_{H1H2}$. The worst case is when $^nJ_{H1H2} = 6.25$ Hz where signals for which $^nJ_{CH}$ are between 12 and 26 Hz are basically negligible. However, analysis shows that some of the lost magnetization is actually transferred to the second proton; this means some of magnetization from the second proton may be transferred to the first proton in a similar fashion. Moreover, if heteronuclear coupling between the carbon and the second proton is significant, substantial amounts of magnetization from the first proton may be recovered. This mechanism is actually a different type of relay transfer, allowing cross peaks to appear for CH fragments through a third spin (second proton).

RESULTS AND DISCUSSION

Sodium Acrylate and Acetic Acid

The efficiencies of LR-J-HSMQC experiments were first tested on sodium acrylate (**1**) and acetic acid (**2**) solutions. Sodium acrylate was chosen because its carboxyl carbon displays a wide range of long-range J_{CH} values, $^3J_{C1H3b} = 14.1$ Hz, $^3J_{C1H3a} = 7.6$ Hz, and $^2J_{C1H2} = 4.1$ Hz (*14*). Proton–proton scalar couplings are also significant, with $^3J_{H3aH2} = 17.2$ Hz and $^3J_{H3bH2} = 10.5$ Hz (*15*). Acetic acid, on the other hand, represents an isolated CH_3 fragment, $^2J_{C1H2} = -6.7$ Hz (*16*), and no homonuclear coupling.

Figure 4 displays f_2 slices from the D-HMBC and LR-J-HSMQC spectra, optimized for $J = 6.25$ Hz ($\tau = 80$ ms), of sodium acrylate and acetic acid. As shown, the D-HMBC(80) experiment gave very intense H3a/C1 ($^nJ_{CH} = 7.6$ Hz) and H2/C1 ($^nJ_{CH} = 4.1$ Hz) cross peaks; however, the H3b/C1 ($^nJ_{CH} = 14.1$ Hz) cross peak was missing. The absence of this cross peak was not surprising given that the D-HMBC(80) profile has an excitation null at $^nJ_{CH} = 12.5$ Hz. Theoretically, the LR-J-HSMQC(80,27) and LR-J-HSMQC(27,80) experiments (Fig. 2C) should provide better excitation than D-HMBC(80) at $^nJ_{CH} = 14.1$ Hz (∼87%) while leaving the excitation for $^nJ_{CH} = 4.1$ and 7.6 Hz virtually unchanged. As shown in Fig. 4, LR-J-HSMQC(80,27) spectra showed reasonably intense H3a/C1 and H2/C1 cross peaks and a medium-intensity H3b/C1 cross peak while the LR-J-HSMQC(27,80) spectra yielded medium-intensity H3a/C1 and H2/C1 cross peaks and an intense H3b/C1 cross peak. It is evident that both LR-J-HSMQC experiments were successful in yielding the H3b/C1 cross peak for which $^nJ_{CH} = 14.1$ Hz. This clearly establishes the effectiveness of LR-J-HSMQC experiments for detecting correlations that may be missed in a conventional long-range heteronuclear shift-correlation experiment.

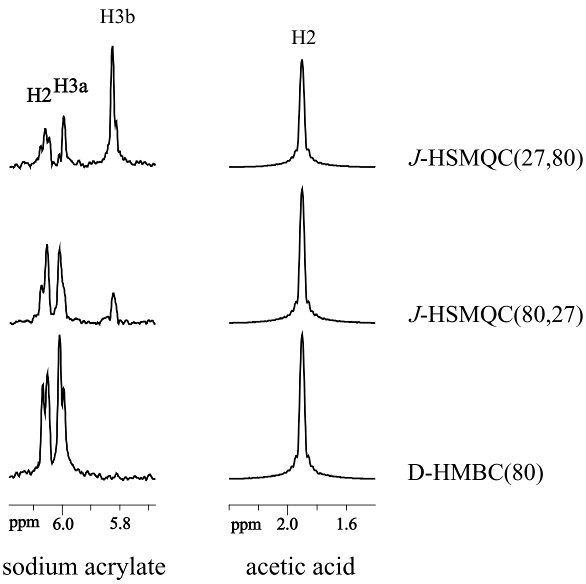

FIG. 4. Selected f_2 slices from 2D maps of D-HMBC(80), LR-J-HSMQC(80,27), and LR-J-HSMQC(27,80) of sodium acrylate (**1**) and acetic acid (**2**). Each slice corresponds to the carboxyl carbon of the appropriate test molecule. The f_2 slices for each compound are plotted at the same absolute intensity.

The intensities of H3a/C1 and H2/C1 cross peaks in the LR-J-HMQC spectra were significantly weaker than those in D-HMBC(80). Relaxation and pulse imperfections could decrease the expected signal intensity but it is likely that this big decrease in signal intensity was due to evolution of homonuclear coupling that occurred during the extra delay period τ'. This was supported by the fact that in sodium acetate, in which there is no ^1H–^1H coupling, the decrease in the long-range H2/C1 signal intensity in J-compensated experiments,

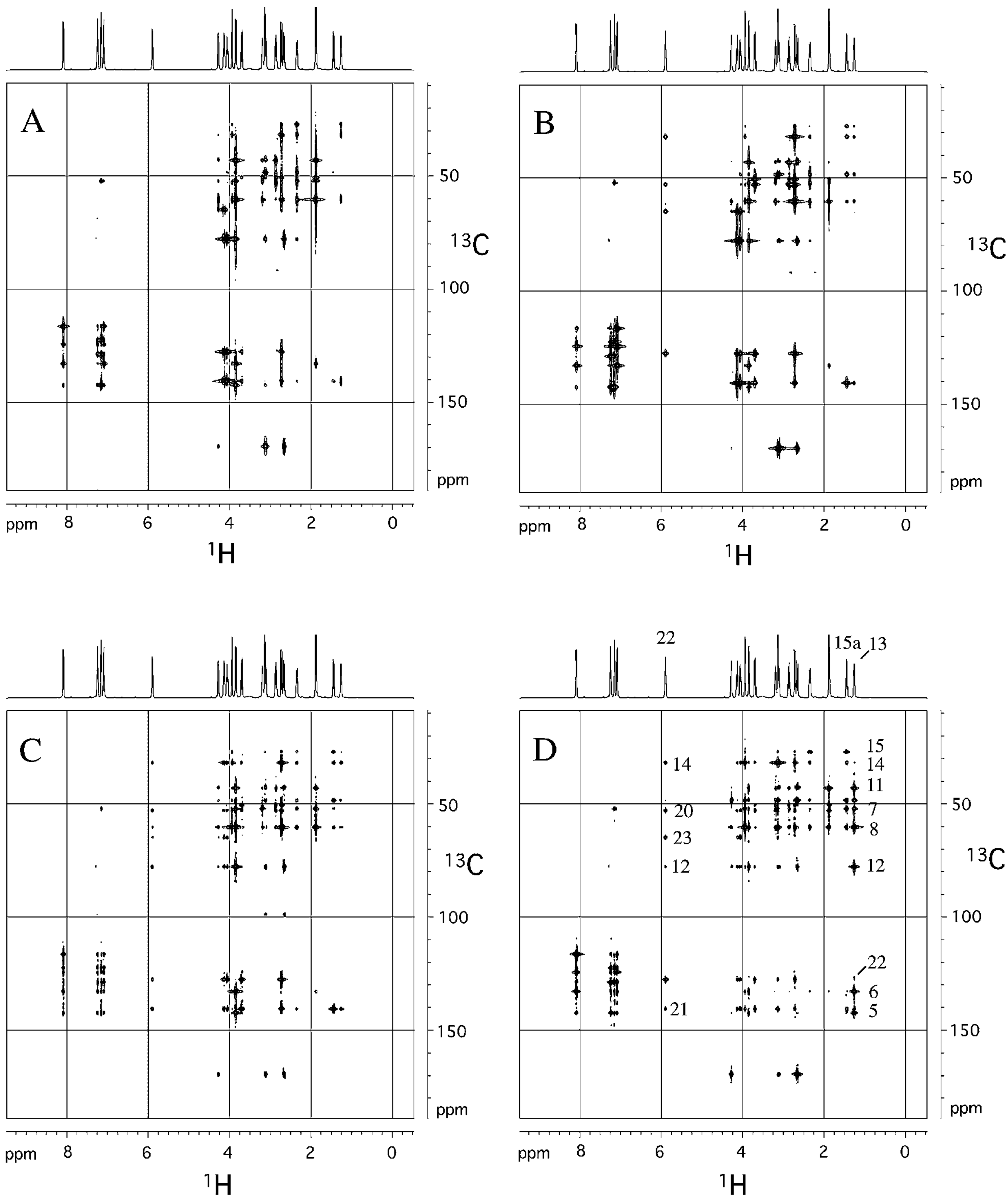

FIG. 5. ^{1}H–^{13}C 2D maps of strychnine (**3**) obtained using (A) D-HMBC(80), (B) D-HMBC(60), (C) LR-*J*-HSMQC(80,27), and (D) LR-*J*-HSMQC(27,80) pulse sequences. All maps were plotted with the same vertical scaling factor. Cross peaks of interest are labeled in (D), where the numbers refer to the atoms in structure **3**.

as compared to D-HMBC(80), was relatively small, ∼10% for LR-*J*-HSMQC(80,27) and ∼25% for LR-*J*-HSMQC(27,80); this outcome is very acceptable. Such a decrease in the signal due to homonuclear coupling was not realized in the original *J*-HSMQC for direct correlations (*8*), because the delays employed were sufficiently short to inhibit homonuclear coupling effects. Although this might be perceived as a drawback of the long range *J*-HSMQC sequence in comparison to some conventional sequences, the homonuclear proton coupling effects can be exploited to produce relay-type cross peaks to establish connectivities over more than three bonds. These advantages are demonstrated in the LR-*J*-HSMQC spectra of a more complex molecule, strychnine.

Strychnine

Figure 5 presents D-HMBC and LR-*J*-HSMQC spectra of strychnine. Although the sensitivities of the *J*-compensated experiments are slightly lower for some correlations, the spectra reveal a considerably larger number of correlations than are seen for the conventional spectra, especially that of D-HMBC(80). This is exemplified by cross peaks with proton chemical shifts at 1.26 ppm (H13), 1.44 ppm (H15a), and 5.92 ppm (H22) which are clearly "scarce" in the D-HMBC(80) spectrum.

There was a large difference in the performance of the two *J*-compensated experiments, as shown by the variation of cross peak intensities. For correlations observed in both spectra, the signal intensity of D-HMBC(80) was closer to that of LR-*J*-HSMQC(80,27) than to that of LR-*J*-HSMQC(27,80). This pattern of behavior was similar to that observed in sodium acrylate as presented above. In addition, there were cross peaks which were very intense in the LR-*J*-HSMQC(27,80) spectrum which were absent or not as intense in the LR-*J*-HSMQC (80,27) spectrum. Closer inspection showed some of these intense cross peaks were expected to have low $^nJ_{CH}$ values. These included the two-bond correlation, H13/C12 ($^2J_{CH} \sim 1.2$ Hz) (*18*), and four-bond correlations, H13/C5 and H13/C6. Clearly, these cross peaks are likely to be due to relay effects. As mentioned above, LR-*J*-HSMQC(27,80) is expected to show more relay cross peaks than LR-*J*-HSMQC(80,27). The appearance of this type of cross peak may be beneficial since they have additional information that would not normally appear in the conventional D-HMBC experiment. Care has to be taken, however, in relating their intensities to $^nJ_{CH}$ coupling values because some two-bond and four-bond correlations are more intense than their three-bond counterparts. Often, the observation of two-bond and three-bond interactions is enough to determine CH connectivities so that the additional four-bond correlations could only

TABLE 1
Performance of Various Experiments for Detection of Selected Long-Range Correlations in Strychnine[a]

	Experiment[b]						
Correlation	D-HMBC(80)	D-HMBC(60)	LR-*J*-HSMQC(80,27)	LR-*J*-HSMQC(27,80)	ACCORD-HMBC	*J*-IMPEACH-MBC	GSQMBC
a) H13/							
C14	+	+	+	+	+	+	+
C8	+	+	+	+	+	+	+
C12	w	−	+	+	+	−	+
C15	+	+	+	−	+	+	+
C11	−	−	+	+	−	−	+
C7	−	−	−	+	−	−	+
C21	+	+	+	+	+	+	+
C5	−	−	−	+	−	−	−
C6	−	−	−	+	−	−	−
C22	−	−	+	+	−	−	−
b) H22/							
C23	w	+	+	+	−	−	+
C21	−	−	+	+	−	−	+
C14	−	+	+	+	−	−	+
C20	w	+	+	+	−	+	+
C12	−	+	+	+	−	−	−
c) H15a/							
C14	+	+	+	+	+	+	+
C16	−	+	+	+	+	+	+
C13	+	+	+	+	+	+	+
C7	−	−	+	+	+	+	+
C21	+	+	+	+	+	+	+

[a] Strong and medium intensity cross peaks are denoted by +, weak intensity cross peaks by w, and unobserved by −.
[b] D-HMBC and LR-*J*-HSMQC data are from this study, ACCORD-HMBC data correspond to those reported by Martin *et al.* (*3*) while *J*-IMPEACH-MBC and GSQMBC data correspond to those reported by Marquez *et al.* (*18*).

complicate the structural analysis. There are however many instances where the observation of a four-bond correlation may be particularly useful.

In Table 1 we compare the performance of various long-range heteronuclear shift correlation experiments for selected protons in strychnine. Since this molecule had been used as a test compound for ACCORD-HMBC (*3*), *J*-IMPEACH-MBC (*17, 18*), and GSQMBC (*18*), it is instructive to consider the results from these methods for comparison. Note that the data included here should only serve as a rough guide to relative performance since there are many differences in experimental conditions, such as magnetic field strength, temperature, probe performance, sample concentration, and other acquisition parameters. It is clear from Table 1 that D-HMBC(80) was the least efficient in producing long-range correlations while LR-*J*-HSMQC(27,80) was the most efficient. GSQMBC (*19*), which utilizes carbon single-quantum coherence during t_1 evolution and does not refocus proton magnetization, appears to be very impressive yielding more of the selected correlations than the ACCORD-HMBC optimized for $^nJ_{CH} = 2$–25 Hz and *J*-IMPEACH-MBC. This is probably due to the fact that the single-quantum coherences are not prone to degradation due to homonuclear coupling during t_1 and that GSQMBC is shorter in duration than all other experiments considered here. Since part of the coherences in LR-*J*-HSMQC experiments also evolve as carbon single-quantum during t_1, it is likely that the *J*-compensated experiments also benefit from the same favorable effect. Clearly, the use of single-quantum coherences, instead of multiple-quantum coherences, during t_1 is advantageous in long-range heteronuclear shift correlation studies.

CONCLUSIONS

We have presented here the results of an investigation into the optimization of the *J*-HSMQC experiment for use in long-range heteronuclear shift-correlation studies. We have proposed two *J*-compensated experiments, LR-*J*-HSMQC(80,27) and LR-*J*-HSMQC(27,80), which are effective for $^nJ_{CH}$ values above 3 Hz. The beneficial property of LR-*J*-HSMQC in showing both relay and long-range peaks could be potentially useful in establishing connectivities in many molecules. LR-*J*-HSMQC(27,80), in particular, was found to be efficient in yielding four-bond correlations by relay magnetization transfer. In practice, LR-*J*-HSMQC experiments are more susceptible to homonuclear coupling modulation, relaxation effects, and pulse imperfections than the conventional D-HMBC; this is due to the extra τ' delays and RF pulses in the sequences. However, their efficiency in enhancing signals in the presence of a wide range of $^nJ_{CH}$ values as a consequence of their more uniform excitation profiles could in many instances compensate for this shortcoming.

EXPERIMENTAL

Experiments were performed on a Bruker Avance DRX-600 spectrometer using a 5-mm broadband inverse detection probehead with triple axis gradient coil operating at 25°C. Gradient values of 40 : −40 : 10 as shown in Fig. 1 correspond to the percentage of the maximum z-gradient of 70 G cm^{-1}. The HMQC pulse sequence referred to as "inv4gp" in Bruker standard pulse program terminology was used for D-HMBC. Gradient ratios employed for this pulse sequence were 50 : 30 : 40. The 90° pulse lengths were typically 12 μs for protons and 10 μs for ^{13}C. Sample compounds were 50 mg sodium acrylate (**1**) in 0.5 mL D_2O, 50% (v/v) acetic acid (**2**) in D_2O, total volume of 0.5 mL, and 70 mg strychnine (**3**) in 1 mL $CDCl_3$, in a sealed NMR tube. In all experiments, 4 dummy scans were performed prior to acquisition, and either 2 or 4 scans were collected per t_1 increment. No low-pass J-filters or purging sequences that remove one-bond correlations were implemented.

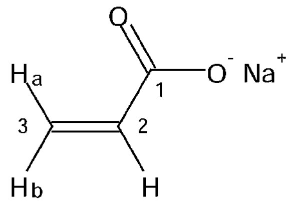

1

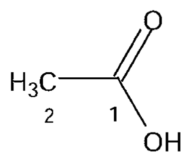

2

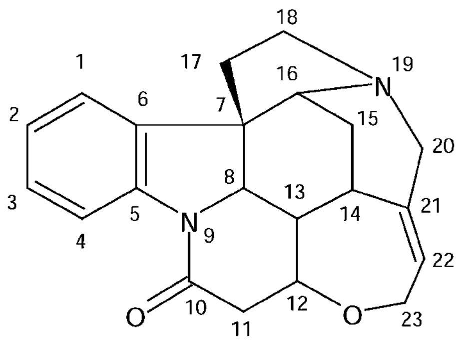

3

For the sodium acrylate experiment, 2D data sets consisted of 256 × 8 increments covering spectral widths of 610 Hz (^{1}H) and 13,580 Hz (^{13}C); for the acetic acid experiment, data sets were 256 × 32 increments spanning 898 Hz (^{1}H) and 15,090 Hz (^{13}C); and for the strychnine experiment, data sets were 2 K × 256 increments spanning 6010 Hz (^{1}H) and 27165 Hz (^{13}C). Data sets were apodized with a cosine function in both dimensions and were zero-filled to obtain a final data matrix of 512 × 256 for sodium acrylate and acetic acid, and 2048 × 512 for strychnine. All spectral data were processed in magnitude mode.

ACKNOWLEDGMENTS

We thank Mr. Bill Lowe for technical assistance. This work was supported by an Australian Research Council Grant to P.W.K.

REFERENCES

1. A. Bax and M. F. Summers, ^{1}H and ^{13}C assignments from sensitivity-enhanced detection of heteronuclear multiple-bond connectivity by 2D multiple quantum NMR, *J. Am. Chem. Soc*. **108,** 2093–2094 (1986).
2. R. Wagner and S. Berger, ACCORD-HMBC: A superior technique for structural elucidation, *Magn. Reson. Chem.* **36,** S44–S46 (1998).
3. G. E. Martin, C. E. Hadden, R. C. Crouch, and V. V. Krishnamurthy, ACCORD-HMBC: Advantages and disadvantages of static vs. accordion optimization, *Magn. Reson. Chem.* **37,** 517–528 (1999).
4. C. E. Hadden, G. E. Martin, and V. V. Krishnamurthy, Improved performance accordion heteronuclear multiple-bond correlation spectroscopy-IMPEACH-MBC, *J. Magn. Reson*. **140,** 274–280 (1999).
5. C. E. Hadden, G. E. Martin, and V. V. Krishnamurthy, Constant time inverse-detection gradient accordion rescaled heteronuclear multiple bond correlation spectroscopy: CIGAR-HMBC, *Magn. Reson. Chem.* **39,** 143–147 (2000).
6. K. Furihata and H. Seto, 3D-HMBC, a new technique useful for structural studies of complicated molecules, *Tetrahedron Lett*. **37,** 8901–8902 (1996).
7. K. Furihata and H. Seto, Decoupled HMBC(D-HMBC), an improved technique of HMBC, *Tetrahedron Lett*. **36,** 2817–2820 (1995).
8. A. M. Torres, T. T. Nakashima, and R. E. D. McClung, J-Compensated proton detected heteronuclear shift-correlation experiments, *J. Magn. Reson. A* **102,** 219–227 (1993).
9. A. M. Torres and R. E. D. McClung, J-Compensated DEPT sequences, *J. Magn. Reson.* **92,** 45–63 (1991).
10. A. M. Torres, T. T. Nakashima, and R. E. D. McClung, Improved J-compensated APT experiments, *J. Magn. Reson. A* **101,** 285–294 (1993).
11. S. Wimperis and G. Bodenhausen, Heteronuclear coherence transfer over a range of coupling constants: A broadband-INEPT experiment, *J. Magn. Reson.* 264–282 (1986).
12. A. M. Torres, T. T. Nakashima, and R. E. D. McClung, Improvement of INADEQUATE using compensated delay and pulses, *J. Magn. Reson.* **99,** 99–117 (1992).
13. L. Lerner and A. Bax, Sensitivity-enhanced two-dimensional heteronuclear relayed coherence transfer NMR spectroscopy, *J. Magn. Reson.* **69,** 375–380 (1986).
14. E. Breitmaier and W. Voelter, "Carbon-13 NMR Spectroscopy," 3rd ed., VCH, Weinheim (1987).
15. W. Brügel, "Handbook of NMR Spectral Parameters," Vol. 2, Heyden, London (1979).
16. H.-O. Kalinowski, S. Berger, and S. Braun, "Carbon-13 NMR Spectroscopy," Wiley, Chichester (1988).
17. R. T. Williamson, B. L. Marquez, W. H. Gerwick, G. E. Martin, and V. V. Krishnamurthy, J-IMPEACH-MBC: A new concatenated NMR experiment for F_1 scalable, J-resolved HMBC, *Magn. Reson. Chem.* **39,** 127–132 (2001).
18. B. L. Marquez, W. H. Gerwick, and R. T. Williamson, Survey of NMR experiments for the determination of $^{(n)}J$(C,H) heteronuclear coupling constants in small molecules, *Magn. Reson. Chem.* **39,** 499–530 (2001).
19. R. Marek, L. Králík, and V. Sklenár, Gradient-enhanced HSQC experiments for phase-sensitive detection of multiple bond interactions, *Tetrahedron Lett.* **38,** 665–668 (1997).